Neoplasia • Vol. 8, No. 2, February 2006, pp. 89–95 89

www.neoplasia.com

Lowering of Tumor Interstitial Fluid Pressure Reduces Tumor Cell Proliferation in a Xenograft Tumor Model[1]

Matthias Hofmann[*,†], Maike Guschel*[*], August Bernd*[*], Jürgen Bereiter-Hahn*[†], Roland Kaufmann*[*], Christa Tandi*[‡], Helge Wiig*[§] and Stefan Kippenberger*[*]

*Department of Dermatology and Venerology, University Hospital, Johann Wolfgang Goethe University, Frankfurt/Main D-60590, Germany; †Kinematic Cell Research Group, Department of Zoology, Johann Wolfgang Goethe University, Frankfurt/Main D-60439, Germany; ‡Central Research Facility, University Hospital, Johann Wolfgang Goethe University, Frankfurt/Main D-60590, Germany; §Department of Biomedicine, Section of Physiology, University of Bergen, Bergen N-5009, Norway

Abstract

High tumor interstitial fluid pressure (TIFP) is a characteristic of most solid tumors. TIFP may hamper adequate uptake of macromolecular therapeutics in tumor tissue. In addition, TIFP generates mechanical forces affecting the tumor cortex, which might influence the growth parameters of tumor cells. This seems likely as, in other tissues (namely, blood vessels or the skin), mechanical stretch is known to trigger proliferation. Therefore, we hypothesize that TIFP-induced stretch modulates proliferation-associated parameters. Solid epithelial tumors (A431 and A549) were grown in Naval Medical Research Institute nude mice, generating a TIFP of about 10 mm Hg (A431) or 5 mm Hg (A549). Tumor drainage of the central cystic area led to a rapid decline of TIFP, together with visible relaxation of the tumor cortex. It was found by sodium dodecyl sulfate polyacrylamide gel electrophoresis and Western blot analysis that TIFP lowering yields a decreased phosphorylation of proliferation-associated p44/42 mitogen-activated protein kinase and tumor relaxation. In confirmation, immunohistochemical staining showed a decrease of tumor-associated proliferation marker Ki-67 after TIFP lowering. These data suggest that the mechanical stretch induced by TIFP is a positive modulator of tumor proliferation.

Neoplasia (2006) **8,** 89–95

Keywords: Tumor interstitial fluid pressure, tumor cell proliferation, mechanical stimuli, p44/42 MAPK, Ki-67.

Introduction

It is a common observation that interstitial fluid pressure is elevated in both human and experimental solid tumors compared to normal tissues [1–3]. Enhanced tumor interstitial fluid pressure (TIFP) is mainly the result of a richly developed and highly permeable vascular network, combined with facilitated transendothelial fluid transfer [4,5]. Furthermore, the lack of a functional lymphatic system and the abnormal vasculature in the tumor area give rise to hypertension [6–8]. Clinically, a high TIFP is marked by a reduced delivery and uptake of anticancer drugs or macromolecules and, hence, lack of therapeutic effects [9].

In addition, vascular and interstitial fluid pressure may be considered to result in permanent stretching stimulation to the tumor cortex. As mechanical stretch has been identified as a trigger factor supporting cell proliferation in other tissues, it seems likely that the TIFP also triggers tumor cell proliferation [10–14]. This assumption is backed by findings demonstrating the activation of mitogen-activated protein kinase (MAPK) in response to mechanical stimuli in various cell lines, suggesting a ubiquitous reaction to mechanical stress [15–17]. In particular, mechanical stretch displayed a strong activation of p44/42 MAPK—a key regulator in proliferation-associated signaling—in epithelial cells [12,13,18]. There is a huge body of evidence indicating that surface receptors of the integrin family convey the phosphorylation and activation of MAPKs through EGFR transactivation [12,19–21].

The proliferative nature of mechanical stretch is further evidenced by studies regarding cell count and the expression of the nuclear antigen Ki-67 [22,23]. Ki-67 is expressed in all phases of the cell cycle, except in the G_0 phase, and serves as a gold standard in tumor diagnosis [24,25]. In various hyperproliferative diseases, the expression of Ki-67 and the activation of p44/42 MAPK were found to be closely correlated [26,27].

In the present study, the mechanical aspect of TIFP in solid tumors during tumor cell proliferation was investigated for the first time. We hypothesized that, by lowering TIFP, mechanical relaxation of the tumor cortex controls proliferation-relevant effectors such as p44/42 MAPK and Ki-67.

Abbreviations: TIFP, tumor interstitial fluid pressure; MAPK, mitogen-activated protein kinase

Address all correspondence to: Matthias Hofmann, Department of Dermatology and Venerology, University Hospital, Theodor-Stern Kai 7, Frankfurt/Main D-60590, Germany. E-mail: matthias.hofmann@em.uni-frankfurt.de

[1]This work was supported by grants from Dr. August Scheidel Stiftung (to M.H.) and Volkswagenstiftung (grant I/77 731; to S.K.).

Received 15 July 2005; Revised 10 November 2005; Accepted 11 November 2005.

DOI 10.1593/neo.05469

Materials and Methods

Animals and Experimental Tumors

Female Naval Medical Research Institute (NMRI) nude mice (5–6 weeks, 20–24 g; Janvier Elevage, Le Genest St. Isle, France) were subcutaneously implanted with 2-mm^3 tissue fragments of A431 epidermoid vulva carcinoma or A549 lung carcinoma. Both epithelial tumors featured a cystic nature with viable tissue only in the periphery and a central area filled with vascular fluid and necrotic cells.

Mice were kept under specific pathogen-free conditions. Sterilized food and tap water were given *ad libitum*. Animals were anesthesized with ketamine/xylazine (100/10 mg/kg, i.p.; Pharmacia, Erlangen, Germany/BayerVital, Leverkusen, Germany). During anesthesia administration, mice were placed on a regulated heating pad to keep the body temperature at 38 to 39°C. At the end of the experiments, anesthesized mice were sacrificed by cervical dislocation.

Tumor size was measured with calipers every 3 days, starting 7 days after implantation of tumor fragments, and tumor volume was calculated as described previously [28]. TIFP was evaluated using the "wick-in-needle" technique in the central cystic area and was related to tumor volume [29]. Fluid communication between the needle and the tumor tissue was tested by compressing and decompressing the tubing, and data were accepted only if the recorded pressure returned rapidly to the value prior to tube compression. TIFP measurement began at a tumor volume of 500 mm^3. After tumor puncture using a hollow needle (15 G), the TIFP equaled control measurements in the subcutis (0 to −1 mm Hg). To detect changes in MAPK phosphorylation, tumors were excised 5 minutes, 10 minutes, 30 minutes, 60 minutes, and 6 hours after puncture. Changes in Ki-67 expression were evaluated in tumor specimens excised after 24 hours. To avoid reinflation of the tumor, a redon-mini drain system (pfm, Cologne, Germany) was applied. The suction bellow of the redon-mini drain was fixed to a crane device (CMA Microdialysis, Solna, Sweden) to allow free movement of mice. All animal experiments were approved in accordance with German animal welfare regulations.

Immunoblotting

For analysis of mechanically induced MAPK activation, tumor tissue was homogenized in cell lysis buffer (Cell Signaling Technology, Frankfurt/Main, Germany) using an ultrathurax (IKA, Staufen, Germany). After sonication and centrifugation, the protein concentration of the supernatant was determined (DC Protein Assay Kit; BioRad, Munich, Germany) and standardized using bovine serum albumin (BSA). Equal protein amounts (10 μg) were mixed with 3× sodium dodecyl sulfate (SDS) sample buffer [187.5 mM Tris–HCl (pH 6.8), 6% SDS, 30% glycerol (water-free), 150 mM DTT, and 0.3% bromophenol blue–Na] and separated by electrophoresis on 12% SDS–polyacrylamide gels. For immunoblotting, proteins were transferred to PVDF membranes (Roth, Karlsruhe, Germany). The membranes were placed in blocking buffer [Tris-buffered saline (pH 7.6), 0.1% Tween-20, and 5% BSA] for at least 1 hour, followed by overnight incubation with primary antibodies in blocking buffer at 4°C. Phosphorylation of p44/42 was detected using a phosphospecific antibody (Thr202/Tyr204; Cell Signaling Technology). Detection of total p44/42 (Cell Signaling Technology) served as loading control. Bound primary antibodies were detected with secondary antibodies coupled to horseradish peroxidase (antirabbit; Cell Signaling Technology) and visualized with LumiGlo detection system (Cell Signaling Technology).

Immunohistochemical Staining

Tumors were fixed in 4% paraformaldehyde, dehydrated, embedded in paraffin, and cut using a Leica RM2125 rotary microtome (Leica Microsystems, Wetzlar, Germany). Before staining, tumor slides were dried for 15 minutes at 65°C, dewaxed in xylene, and rehydrated in graded alcohols, followed by heat-induced epitope retrieval in 10 mM citrate buffer (pH 6.0; DakoCytomation, Hamburg, Germany). After cooling the specimen for 20 minutes, tissue slides were washed [H_2O_2/methanol, 0.1% Triton–phosphate-buffered saline (PBS), and 2% glycin–PBS] and incubated for 10 minutes with a protein-blocking agent (Immunotech, Marseilles, France). Then the slides were incubated with anti–human Ki-67 (clone MIB-1, 1:50; DakoCytomation) in PBS for 1 hour at room temperature. After three washes in PBS, slides were incubated with a biotinylated secondary antibody and a streptavidin peroxidase reagent (Immunotech) for 45 minutes. Staining was performed using AEC peroxidase substrate kit (Vector Laboratories, Burlingame, CA). Sections were counterstained with Mayer's hematoxylin (AppliChem, Darmstadt, Germany). Control staining was performed in the absence of primary or secondary antibody, respectively. Photographs were taken by a Sony Cyber Shot 3.3 (Sony Deutschland, Cologne, Germany) connected to a Zeiss Axioskop (Zeiss, Oberkochen, Germany). Ki-67 index was calculated as the number of positive nuclei per 1000 nuclei. Approximately 1000 nuclei (890–1100) were counted in the viable rim area of 14 tumor slides of both tumor entities (7× control, 7× drained tumors). Quantitative analysis was performed using CellExplorer 2000 Software (BioSciTec, Frankfurt/Main, Germany).

Immunofluorescent staining against CD31 was performed according to the manufacturer's instructions in acetone-fixed frozen tumor sections using purified anti–mouse CD31-PE antibody (clone 390, 1:200; Acris Antibodies, Hiddenhausen, Germany).

Results

NMRI nude mice were subcutaneously transplanted into the left and right parts of the back with fragments of A431 or A549 tumors. The measurement of tumor volume was started 7 days after tumor fragments had been implanted. Volumetric growth rate differed significantly between both tumor entities. A tumor volume of 2000 mm^3 was reached after 15 days in A431 tumors, and after 27 days in A549 tumors (Figure 1*A*). TIFP was evaluated every 3 days, starting after tumors had reached a volume of approximately

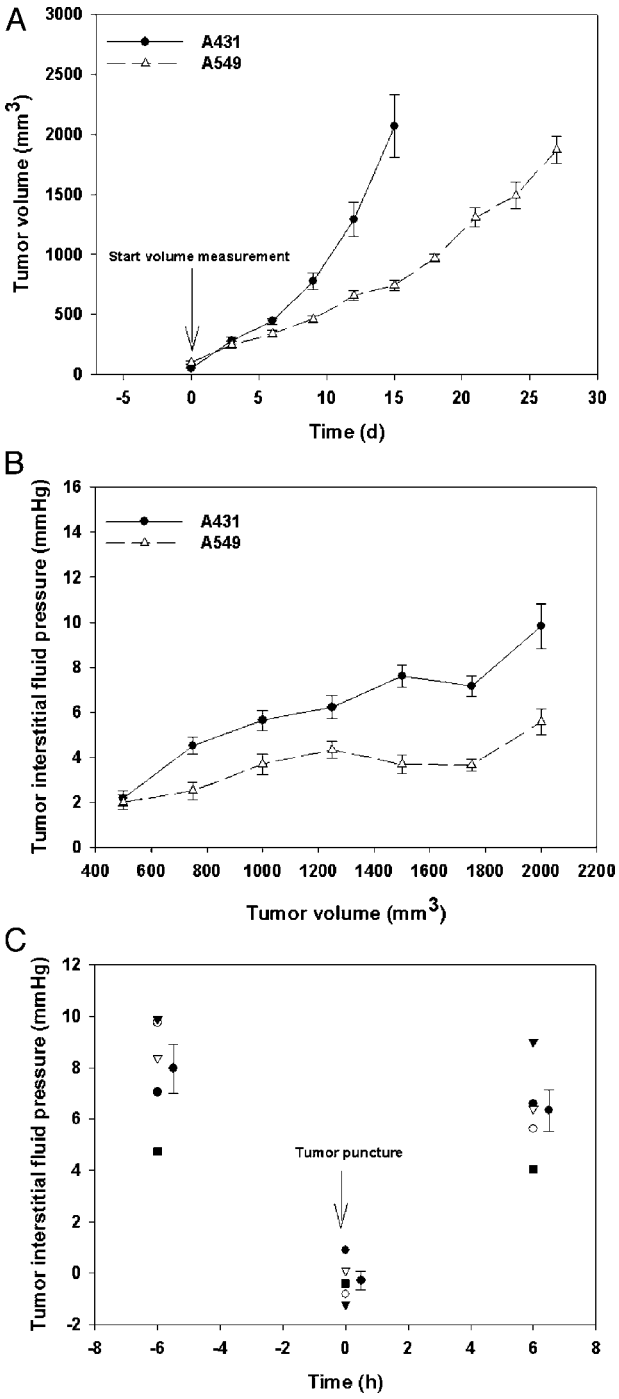

Figure 1. *Tumor volume and TIFP in A431 and A549 tumors in NMRI nude mice. (A) Increase of tumor volume after implantation of small fragments (2 mm^3) of A431 or A549 tumors. The plots represent tumor volume versus time. (B) Effect of increasing tumor volume on the TIFP. (C) Effect of tumor puncture on the TIFP. Scatter plots show the TIFP of five individual animals 6 hours before, during, and 6 hours after tumor puncture. Plots in (A) and (B) show the results of n = 10 (A431/A549). Plots in (C) show results of n = 5 (A431) (mean ± SE).*

500 mm^3. In A431 tumors, TIFP increased constantly with increasing tumor volume. At a tumor volume of 2000 mm^3, the maximum TIFP averaged 10 mm Hg. In A549 tumors, a more moderate increase in TIFP was measured with maximum values of 5 mm Hg (Figure 1*B*). As shown in Figure 1*C*, TIFP was lowered to −1 to 0 mm Hg after tumor puncture. Control measurements in the subcutis of the mice showed also interstitial fluid pressure values of −1 mm Hg (data not shown). After tumor puncture, TIFP recovered rapidly within 6 hours, reaching TIFP values in the range of the level prior to puncture (Figure 1*C*).

Permanent mechanical stretching, as induced by increased TIFP, was found to influence cell morphology. The mechanical load of the inflated A431 tumor is displayed by a smooth and even surface (Figure 2*A*(*I*)). Puncture of the same tumor resulted in a dramatic reduction in TIFP with tumor collapse (Figure 2*A*(*II*)). A549 tumors showed a similar morphology (data not shown). In a section of an untreated A431 tumor stained with hematoxylin and eosin, three distinct areas are visible: the central necrotic core, the small viable rim of proliferating tumor cells, and the surrounding tumor capsule (Figure 2*B*(*I*)). Tumor cells of the outer tumor cortex displayed expanded morphology. In contrast to the avascular necrotic tumor center, this tissue layer is highly vascularized, vital, and proliferative (Figure 2*B*(*II*)) [30,31].

To characterize molecular signaling cascades driven by TIFP lowering, phosphorylation of p44/42 MAPK was investigated. Tissue samples of tumors were excised at 5 minutes, 10 minutes, 30 minutes, 60 minutes, and 6 hours after tumor puncture and were analyzed for phospho-p44/42 by Western blot analysis. It was found that the reduction of TIFP for 30 and 60 minutes by puncture reduced the phosphorylation of p44/42 MAPK in A431 and A549 tumors (Figure 3*A*). Control tumors showed a significantly stronger phosphorylation of p44/42. Tumors excised 5 or 10 minutes after TIFP lowering showed no significant reduction in

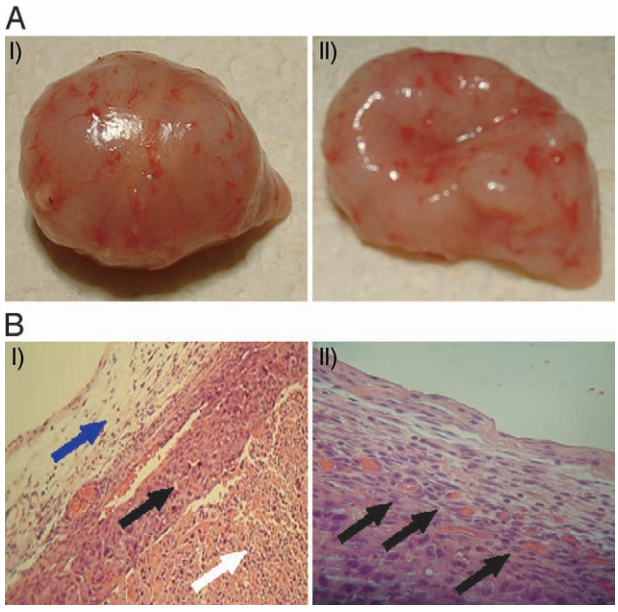

Figure 2. *Effect of puncture on tumor morphology. (A) (I) Untreated A431 control tumor features a tightly inflated tumor cortex. (II) After puncture of the central cystic region, the tumor collapsed, indicating loss of surface tension. (B) Sections from untreated A431 tumors stained with hematoxylin and eosin to highlight mechanically stretched tumor cells. (I) The central necrotic area (white arrow) is surrounded by proliferating tumor tissues (black arrow) and tumor capsule (blue arrow). Original magnification, ×100. (II) Black arrows indicate stretched cells in the proliferative and highly vascularized outer tumor cortex. Original magnification, ×320.*

p44/42 MAPK phosphorylation compared to untreated control tumors (data not shown). In addition, p44/42 MAPK phosphorylation of tumors excised 6 hours after tumor puncture showed similar levels as untreated controls (Figure 3*A*). Data are summarized in Figure 3*B*.

To test whether proliferation is regulated by TIFP reduction, the expression of Ki-67 was evaluated. To enable TIFP lowering for up to 24 hours, a redon-mini drain was implanted in one of the tumors, circumventing the recovery of TIFP for this time period. After 24 hours, mice were sacrificed, and tumors were fixed in paraformaldehyde and embedded in paraffin. The proliferation rate of tumors was determined by immunohistochemical staining against the tumor proliferation marker Ki-67 in A431 and A549 tumors (Figure 4, *A* and *B*). Tumor samples from both tumor entities, drained for 24 hours (Figure 4, *A*(*I*) and *B*(*I*)), showed a reduced expression of human Ki-67 proteins in the proliferating tumor cortex compared to untreated control tumors (Figure 4, *A*(*II*) and *B*(*II*)). The specificity of Ki-67 antibody staining was controlled by withdrawal of the first or secondary antibody, respectively (Figure 4*A*(*III*/*IV*)). An overview of a Ki-67–stained tumor tissue, generated from an untreated control tumor, indicates that only cells from the viable rim were used for Ki-67 index determination (Figure 4*A*(*V*)). The quantitative analysis of Ki-67 expression data showed that Ki-67 expression dropped significantly in drained A431 and A549 tumors compared to the untreated control tumors (Figure 4*C*).

Furthermore, it was tested whether the release of tumor fluid during drainage might destroy vessels in tumor tissues. Staining of drained and untreated tumors with fluorescent-linked antibodies against anti–mouse CD31 (PECAM), a well-known endothelial cell marker, indicated that the vessels in both TIFP-reduced and control tumors are not destroyed and show opened lumina (Figure 5) [32].

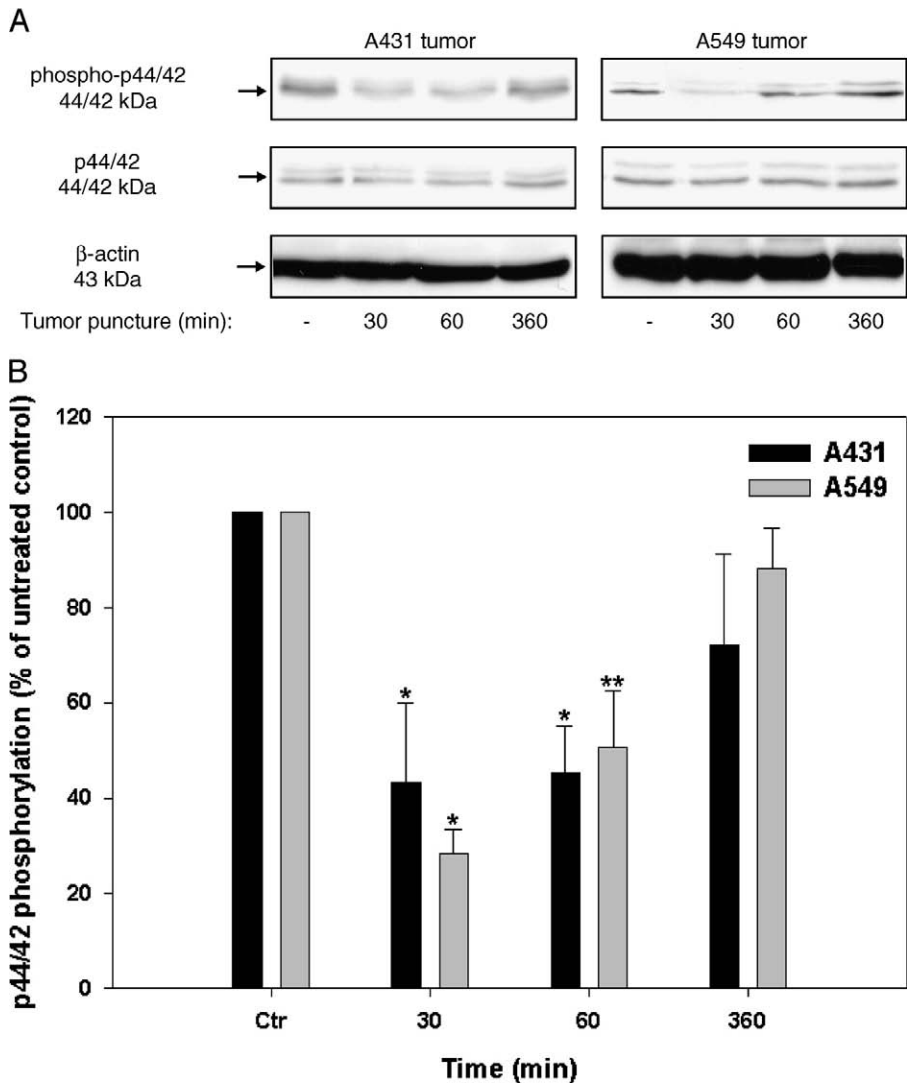

Figure 3. *Reduction of TIFP decreased the phosphorylation of proliferation-associated p44/42 MAPK. (A) Time course of p44/42 phosphorylation in untreated A431 and A549 control tumors and in TIFP-lowered tumors. (B) Quantitative analysis of p44/42 MAPK phosphorylation in TIFP-reduced and control tumors. The values from TIFP-lowered tumors have been normalized to values of control tumors. Data are mean ± SE (*P < .001 vs untreated control tumors; **P < .01 vs untreated control tumors) for five independent experiments.*

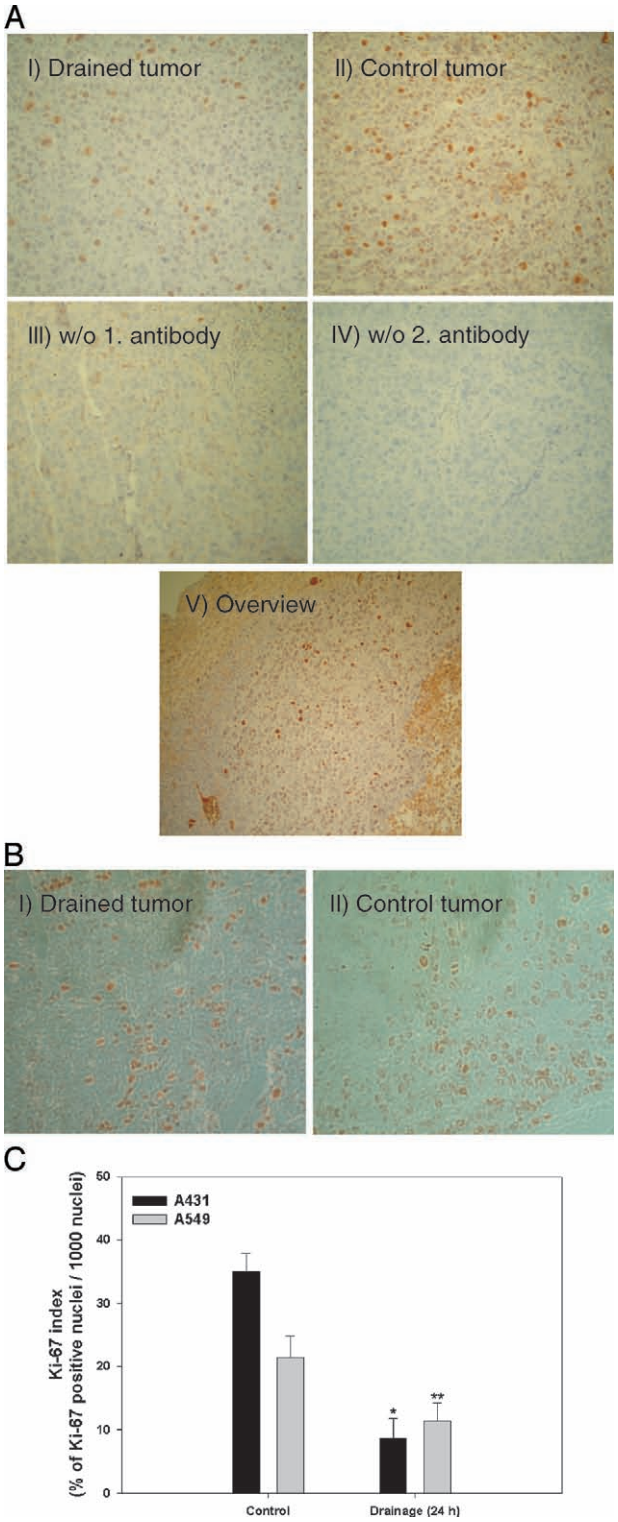

Figure 4. *24-Hour TIFP lowering reduced Ki-67 expression. (A) Immunohistochemical staining of Ki-67 in A431 tumor slides in response to reduced TIFP. (I) Ki-67 expression in TIFP-reduced tumor tissue. (II) Ki-67 expression in untreated control tumors. (III/IV) control staining after withdrawal of the first or secondary antibody. (V) Overview of a tissue slide of a control tumor stained against Ki-67. Original magnification, ×240 (I–IV) and ×100 (V). (B) Immunohistochemical staining of Ki-67 in A549 tumor slides in response to lowered TIFP. (I) Ki-67 expression in TIFP-lowered tumor tissue. (II) Ki-67 expression in untreated control tumors. Original magnification, ×240. (C) Summarized graphical representation of Ki-67 expression. A significant reduction in Ki-67 expression is visible in TIFP-lowered A431 and A549 tumors. The results are the mean ± SE of seven tumors (*P < .001 and **P < .05).*

Discussion

TIFP is described as a physical parameter that hampers the uptake of antitumor drugs into tumor tissue [9]. In this respect, therapeutic approaches lowering TIFP provide improvement of drug delivery [33–35]. Furthermore, enhanced TIFP and compressive forces generated by proliferating tumor cells may lead to a permanent mechanical stretching of the tumor cortex [36]. Nevertheless, a direct compression of cortical tumor cells seems to be unlikely in a hydrostatic system. The present study is driven by the hypothesis that modulation of mechanical load within the central cystic area by reduction of TIFP triggers proliferation-relevant parameters.

In a first step, the TIFP in A431 and A549 tumors was measured and related to tumor volume. Particularly, A431 tumors indicate a strong correlation between TIFP and tumor volume. These results are in concert with previously published data showing that TIFP increases with tumor volume in other tumor species [37–39]. Interestingly, TIFP values of A549 tumors showed only a moderate correlation with tumor growth, indicating that both parameters are not necessarily correlated [40]. Nevertheless, measured TIFP values in A549 tumors were significantly elevated compared to that in subcutaneous tissues. Therefore, it may be assumed that interstitial fluid pressure and compressive forces are responsible for the stretching stimulus. This assumption is backed by immunohistochemical data from A431 tumors indicating that cells of the tumor cortex follow the stretching force vector.

As reviewed by Baxter and Jain [42], most solid tumors are at least in part permeable to fluid flow and do not provide complete fluid retention. Thus, tumor fluid leakage leads to TIFP decrease from the cystic core to the tumor cortex [1]. It is assumed that the drain of tumor fluid is due to TIFP-induced outward convective flux and elevated hydraulic tissue conductivity [41–43]. It is considered that the maintenance of an elevated TIFP originates from the lack of a functional lymphatic system, abnormal vasculature in the tumor area, and interstitial fibrosis [3]. By puncture of the central cystic area, the tumor cortex instantly collapsed and the TIFP was drastically lowered, giving evidence that the TIFP is an important contributor to tumor tension.

It was found that TIFP reduction leads to an immediate decline of p44/42 MAPK phosphorylation in both tumor cell lines within 30 to 60 minutes. Tissue samples analyzed

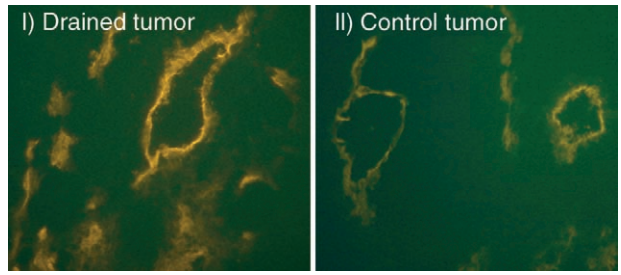

Figure 5. *Reduced TIFP shows no effect on vessel architecture. Immunohistochemical staining of vessels using CD31-PE antibodies in A431 tumor slides. (I) CD31 staining of drained tumors. (II) CD31 staining of control tumors. Original magnification, ×320.*

6 hours after tumor puncture show a recovered phosphorylation pattern of p44/42 MAPK, as seen in control tumors. These data are in concert with our findings that the TIFP recovered quickly within 5 to 6 hours after a single puncture. To study the effects of TIFP release for a longer time span, a redon-mini drainage system was introduced. With this setup, a decrease of Ki-67 expression was demonstrated. The complex changes within the tumor tissue caused by TIFP withdrawal are responsible for measured effects. The concept that TIFP-induced stretching stimulates tumor proliferation is supported by various studies showing that mechanical stretch facilitates cell proliferation *in vitro* [10,12–14]. *In vivo* situations, such as skin enlargement by application of skin expanders or during pregnancy, corroborate the proliferative quality of mechanical stretch [11].

Based on a xenograft tumor model using two different epithelial tumor cell lines, our results suggest that the reduction of mechanical stretch by TIFP lowering reduces tumor proliferation. Therefore, our *in vivo* data are in concert with recently published results from Nathan et al. [44], who showed that elevated physiological pressure enhanced the proliferation of human osteosarcoma cells *in vitro*. Furthermore, it was shown by Salnikov et al. that PGE_1-induced TIFP reduction led to an enhanced drug delivery of 5-fluorouracil and reduced tumor growth. In this model, tumor growth reduction could be described by improved drug uptake and by decreased mechanical tension applied by connective tissue cells and extracellular matrix components [45]. This work is particularly interesting as TIFP lowering is considered to promote mainly convection-driven transport [3]. It was assumed that the uptake of small molecules, such as most chemotherapeutic drugs, is driven by diffusion rather than convection and is, therefore, independent of lowered TIFP [41,42]. The work of Salnikov et al. [35] speaks against this hypothesis as, in their model, the uptake of 5-fluorouracil was enhanced by lowered TIFP. Recently, Heldin et al. [3] reviewed the role of TIFP in drug delivery and hypothesized that tissue changes promote the uptake of small molecules by higher transvascular diffusion. Additionally, the authors hypothesized that convection-driven transport maybe underestimated for small molecules [3].

Therapeutic strategies that simply enable TIFP lowering pose the dilemma that withdrawal of mechanical stretch also promotes interstitial fluid transport and therefore facilitates the uptake of nutrients and growth factors into the tumor [3]. Paradoxically, better nutrition supply should imply increased cell proliferation. However, it has to be mentioned that TIFP lowering enhances drug delivery immediately [35,46]. In contrast, strategies that are based on the destruction of the vasculature by antiangiogenic agents would impair the delivery of drugs to the tumor [47].

As a consequence, a combination of TIFP reduction and simultaneous application of antitumor drugs seems favorable. This approach may offer a two-hit strategy that diminishes stretch-induced proliferation together with enhanced drug supply. In conclusion, our data define TIFP as a trigger factor of tumor proliferation with implications for future therapeutic strategies.

Acknowledgements

We gratefully acknowledge the technical assistance of K. Frank and J. Pfeffer. We also thank A. Runkel for critical review of the manuscript and O. Costa for provision of the CMA Microdialysis device.

References

[1] Jain RK (1994). Barriers to drug delivery in solid tumors. *Sci Am* **271,** 58–65.
[2] Jain RK (1998). The next frontier of molecular medicine: delivery of therapeutics. *Nat Med* **4,** 655–657.
[3] Heldin C-H, Rubin K, Pietras K, and Östman A (2004). High interstitial fluid pressure—an obstacle in cancer therapy. *Nat Rev Cancer* **4,** 806–813.
[4] Boucher Y and Jain RK (1992). Microvascular pressure is the principal driving force for interstitial hypertension in solid tumors: implications for vascular collapse. *Cancer Res* **52,** 5110–5114.
[5] Lee I, Boucher Y, Demhartner TJ, and Jain RK (1994). Changes in tumour blood flow, oxygenation and interstitial fluid pressure induced by pentoxifylline. *Br J Cancer* **69** (3), 492–496.
[6] Carmeliet P and Jain RK (2000). Angiogenesis in cancer and other diseases. *Nature* **407,** 249–257.
[7] Leu AJ, Berk DA, Lymboussaki A, Alitalo K, and Jain RK (2000). Absence of functional lymphatics within a murine sarcoma: a molecular and functional evaluation. *Cancer Res* **60,** 4324–4327.
[8] Netti PA, Berk DA, Swartz MA, Grodzinsky AJ, and Jain RK (2000). Role of extracellular matrix assembly in interstitial transport in solid tumors. *Cancer Res* **60,** 2497–2503.
[9] Jain RK (1987). Transport of molecules in tumor interstitium: a review. *Cancer Res* **47,** 3039–3051.
[10] Takei T, Rivas-Gotz C, Delling CA, Koo JT, Mills I, McCarthy TL, Centrella M, and Sumpio BE (1997). Effect of strain on human keratinocytes *in vitro*. *J Cell Physiol* **173,** 64–72.
[11] Takei T, Mills I, Arai K, and Sumpio BE (1998). Molecular basis for tissue expansion: clinical implications for the surgeon. *Plast Reconstr Surg* **102** (1), 247–258.
[12] Kippenberger S, Bernd A, Loitsch SM, Guschel M, Müller J, Bereiter-Hahn J, and Kaufmann R (2000). Signaling of mechanical stretch in human keratinocytes *via* MAP kinases. *J Invest Dermatol* **114,** 408–412.
[13] Kippenberger S, Loitsch S, Guschel M, Müller J, Knies Y, Kaufmann R, and Bernd A (2005). Mechanical stretch stimulates protein kinase B/Akt phosphorylation in epidermal cells *via* angiotensin II type 1 receptor and epidermal growth factor receptor. *J Biol Chem* **280** (4), 3060–3067.
[14] Silver FH, Siperko LM, and Seehra GP (2003). Mechanobiology of force transduction in dermal tissue. *Skin Res Technol* **9,** 3–23.
[15] Hofmann M, Žaper J, Bernd A, Bereiter-Hahn J, Kaufmann R, and Kippenberger S (2004). Mechanical-pressure induced phosphorylation of p38 mitogen-activated protein kinase in epithelial cells *via* Src and protein kinase C. *Biochem Biophys Res Commun* **316,** 673–679.
[16] Kawabe J, Okumura S, Lee MC, Sadoshima J, and Ishikawa Y (2004). Translocation of caveolin regulates stretch-induced ERK activity in vascular smooth muscle cells. *Am J Physiol Heart Circ Physiol* **286** (5), H1845–H1852.
[17] Yang G, Crawford RC, and Wang JH (2004). Proliferation and collagen production of human patellar tendon fibroblasts in response to cyclic uniaxial stretching in serum-free conditions. *J Biomech* **37** (10), 1543–1550.
[18] Johnson GL and Lapadat R (2002). Mitogen-activated protein kinase pathways mediated by ERK, JNK, and p38 protein kinase. *Science* **298,** 1911–1912.
[19] Ingber DE (1997). Tensegrity: the architectural basis of cellular mechanotransduction. *Annu Rev Physiol* **59,** 575–599.
[20] Moro L, Venturino M, Bozzo C, Silengo L, Altruda F, Beguinot L, Tarone G, and Defilippi P (1998). Integrins induce activation of EGF receptor: role in MAP kinase induction and adhesion-dependent cell survival. *EMBO J* **17** (22), 6622–6632.
[21] Schwartz MA and Ginsberg MH (2002). Networks and crosstalk: integrin signalling spreads. *Nat Cell Biol* **4,** E65–E68.
[22] Takei K, Watanabe H, Itoi T, and Saito T (1996). p53 and Ki-67 immunoreactivity and nuclear morphometry of "carcinoma-in-adenoma" and adenoma of the gall-bladder. *Pathol Int* **46** (11), 908–917.
[23] Kauhanen S, von Boguslawsky K, Michelsson JE, and Leivo I (1998). Satellite cell proliferation in rabbit hindlimb muscle following immobilization

and remobilization: an immunohistochemical study using MIB 1 antibody. *Acta Neuropathol* **95** (2), 165–170.

[24] Gerdes J, Schwab U, Lemke H, and Stein H (1983). Production of a mouse monoclonal antibody reactive with a human nuclear antigen associated with cell proliferation. *Int J Cancer* **31** (1), 13–20.

[25] Scholzen T and Gerdes J (2000). The Ki-67 protein: from the known and the unknown. *J Cell Physiol* **182,** 311–322.

[26] Handra-Luca A, Bilal H, Bertrand JC, and Fouret P (2003). Extracellular signal–regulated ERK-1/ERK-2 pathway activation in human salivary gland mucoepidermoid carcinoma. *J Pathol* **163** (3), 957–967.

[27] Staber PB, Linkesch W, Zauner D, Beham-Schmid C, Guelly C, Schauer S, Sill H, and Hoefler G (2004). Common alterations in gene expression and increased proliferation in recurrent acute myeloid leukemia. *Oncogene* **23** (4), 894–904.

[28] Baumann M, Appold S, Zimmer J, Scharf M, Beuthien-Baumann B, Dubben HH, Enghardt W, Schreiber A, Eicheler W, Petersen C (2001). Radiobiological hypoxia, oxygen tension, interstitial fluid pressure and relative viable tumour area in two human squamous cell carcinomas in nude mice during fractionated radiotherapy. *Acta Oncol* **40** (4), 519–528.

[29] Fadnes HO, Reed RK, and Aukland K (1977). Interstitial fluid pressure in rats measured with a modified wick technique. *Microvasc Res* **14,** 27–36.

[30] Endrich B, Reinhold HS, Gross JF, and Intaglietta M (1979). Tissue perfusion inhomogeneity during early tumor growth in rats. *J Natl Cancer Inst* **62,** 387–395.

[31] Jain RK (1997). Vascular and interstitial physiology of tumours: role in cancer detection and treatment. In Tumour Angiogenesis, Bicknell R, Lewis CE, Ferrara N (Eds). Oxford University Press, Oxford, UK. pp. 45–59.

[32] DeLisser HM, Newman PJ, and Albelda SM (1994). Molecular and functional aspects of PECAM-1/CD31. *Immunol Today* **15** (10), 490–495.

[33] Rubin K, Sjoquist M, Gustafson AM, Isaksson B, Salvessen G, and Reed RK (2000). Lowering of tumoral interstitial fluid pressure by prostaglandin E_1 is paralleled by an increased uptake of ^{51}Cr-EDTA. *Int J Cancer* **86,** 636–643.

[34] Eikenes L, Bruland ØS, Brekken C, and de Lange Davies C (2004). Collagenase increases the transcapillary pressure gradient and improves the uptake and distribution of monoclonal antibodies in human osteosarcoma xenografts. *Cancer Res* **64,** 4768–4773.

[35] Salnikov A, Iversen VV, Koisti M, Sundberg C, Johansson L, Stuhr LB, Sjöquist M, Ahlström H, Reed RK, and Rubin K (2003). Lowering of tumor interstitial fluid pressure specifically augments efficacy of chemotherapy. *FASEB J* **17,** 1756–1758.

[36] Padera TP, Stoll BR, Tooredman JB, Capen D, di Thomaso E, and Jain RK (2004). Pathology: cancer cells compress intratumour vessels. *Nature* **427,** 695.

[37] Boucher Y, Kirkwood JM, Opacic D, Desantis M, and Jain RK (1991). Interstitial hypertension in superficial metastatic melanomas in humans. *Cancer Res* **51** (24), 6691–6694.

[38] Gutmann R, Leunig M, Feyh J, Goetz AE, Messmer K, Kastenbauer E, and Jain RK (1992). Interstitial hypertension in head and neck tumors in patients: correlation with tumor size. *Cancer Res* **52** (7), 1993–1995.

[39] Nathanson SD and Nelson L (1994). Interstitial fluid pressure in breast cancer, benign breast conditions, and breast parenchyma. *Ann Surg Oncol* **1** (4), 333–338.

[40] Boucher Y, Lee I, and Jain RK (1995). Lack of general correlation between interstitial fluid pressure and oxygen partial pressure in solid tumors. *Microvasc Res* **50** (2), 175–182.

[41] Swabb EA, Wei J, and Gullino PM (1974). Diffusion and convection in normal and neoplastic tissues. *Cancer Res* **34,** 2814–2822.

[42] Baxter LT and Jain RK (1989). Transport of fluid and macromolecules in tumors: I. Role of interstitial pressure and convection. *Microvasc Res* **37** (1), 77–104.

[43] Boucher Y, Baxter LT, and Jain RK (1990). Interstitial pressure gradients in tissue-isolated and subcutaneous tumors: implications for therapy. *Cancer Res* **50** (15), 4478–4484.

[44] Nathan SS, DiResta GR, Casas-Ganem JE, Hoang BH, Sowers R, Yang R, Huvos AG, Gorlick R, and Healey JH (2005). Elevated physiologic tumor pressure promotes proliferation and chemosensitivity in human osteosarcoma. *Clin Cancer Res* **11,** 2389–2397.

[45] Berg A, Ekwall AK, Rubin K, Stjernschantz J, and Reed RK (1998). Effect of PGE1, PGI2, and PGF2 alpha analogs on collagen gel compaction *in vitro* and interstitial pressure *in vivo. Am J Physiol* **274,** H663–H671.

[46] Hofmann M, Guschel M, Bernd A, Bereiter-Hahn J, Kaufmann R, Tandi C, and Kippenberger S (2005). Lowering of tumour-interstitial fluid pressure in squamous carcinoma and melanomas enhances the uptake of therapeutics in a xenograft tumour model. *Arch Dermatol Res* **296** (9), 436.

[47] Jain RK (2005). Normalization of tumor vasculature: an emerging concept of antiangiogenic therapy. *Science* **307,** 58–62.